Synthesis and Characterization of Hexasubstituted Cyclotriphosphazene Derivatives with Azo Linking Units

Zuhair Jamain[1*], Melati Khairuddean[2*], Miyeko Lotus Loh[2], Nur Liyana Abdul Manaff[2] and Mohamad Zul Hilmey Makmud[1]

[1]Faculty of Science and Natural Resources, Universiti Malaysia Sabah (UMS), 88400 Kota Kinabalu, Sabah, Malaysia

[2]School of Chemical Sciences, Universiti Sains Malaysia (USM), 11800 Penang, Malaysia

*Corresponding author (e-mail: zuhairjamain@ums.edu.my and melati@usm.my)

A series of new hexasubstituted cyclotriphosphazene derivatives with azo linking units, **4a-d** have been synthesized. The alkylation reaction of 4-acetamidophenol with alkylbromide (heptyl, nonyl, decyl, and dodecyl) formed **1a-d**, which were further reduced to form the corresponding intermediates, **2a-d**. The diazotization reaction of **2a-d** with phenol formed calamitic compounds, **3a-d** with the azo group later reacted with hexachlorocyclotriphosphazene (HCCP) to yield the final compounds, **4a-d**. The functional groups of all the compounds were determined using Fourier Transform Infrared (FTIR), while their molecular structures were characterized by Nuclear Magnetic Resonance (NMR) spectroscopy. The purity of these compounds was confirmed using CHN elemental analysis. Polarized Optical Microscopy (POM) was used to determine the liquid crystal properties of the synthesized compounds. The rod-like intermediates, **3a-d** and the disc-like hexasubstituted final products, **4a-d** were found to be non-mesogenic without any liquid crystal properties. The results showed that the introduction of non-mesogenic intermediate sidearms would eventually give non-mesogenic products. All the final compounds showed the clearing temperature in the range of 120-130°C.

Key words: Hexachlorocyclotriphosphazene; azo; liquid crystal; non-mesogenic; side arm

Received: March 2020; Accepted: September 2020

Over the years, interest in liquid crystalline materials has expanded greatly and the synthesis of these compounds has continued to develop. Molecular shape is important in self-assembly of a molecule which gives the impact on the ordering abilities of mesogenic molecules. The correlation between the molecular structure such as the function of the chain length and type of linking unit is the most important aspect in liquid crystal field. In order to study the effect of the molecular structure on the liquid crystal properties, small changes in the structure can be made while the greater part of the molecular skeleton remains unaltered [1,2]. The influence of different elements and the extended chemical subunits on the molecules allow the construction of the targeted liquid crystal compounds. The molecular shape and the terminal chain length are the key variables in strategies to design new liquid crystal compounds with specific types of molecular organization in a particular range of temperature [3-5].

The phosphorus-nitrogen chemistry, in particular the study of phosphazenes, started since the nineteenth century but has been intensively investigated only in the mid 1950's [6]. Hexachlorocyclotriphosphazene (HCCP), $N_3P_3Cl_6$ is a ring compound consisting of alternating phosphorus and nitrogen atoms with two substituents attached to the phosphorus atoms [7,8]. Much attention has been focused on these interesting compounds because they consist of inorganic backbones as well as organic side-chains [9]. Due to the high reactivity of the P-Cl bond, the corresponding substitution reaction allows the introduction of a wide range of substituents and hence provides numerous hexasubstituted cyclotriphosphazene derivatives with different chemical and physical properties [10-12], as shown in Figure 1.

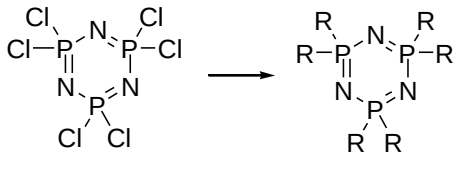

R = can be any nucleophiles

Figure 1. Structures of hexachlorocyclotriphosphazene (left) and its hexasubstituted derivatives

Cyclotriphosphazene core has been widely used in the exploration of the disc-like molecules. Some reported works have revealed that compounds with cyclotriphosphazene core showed excellent liquid crystal properties with different types of linking units attached [13-15]. HCCP derivatives play a role in the ability of the molecules to self-assemble. Dispersion forces are the important contributor to the π-stacked structures due to the increased surface area, which in turn stabilizes the mesophase. One of the important linking units used in this research work is the azo group. Allcock and Klingenberg have reported on the aromatic azo phosphazene polymer liquid crystals [16]. Azo has a functional group of a nitrogen-nitrogen double bond (R_1-N=N-R_2), in between R_1 and R_2 that are bonded to an aryl (aromatic) or alkyl (aliphatic) group. Azo molecules have an elongated, anisotropic geometry which is maintained through the rigidity and linearity of its constituents [17,18]. Two interconnected cyclic rings cause the resulting compound to have a linear planar conformation which will induce the formation of liquid crystals [19]. Today, liquid crystal-based compounds are being used in various applications, such as liquid crystal display [20, 21], flame-retardant materials [22, 23], thermometers [24], optics [25], biosensors [26], and lasers [27].

In this study, a series of calamitic and discotic compounds with azo linking units were synthesized and characterized. Calamitic liquid crystal usually exhibits the nematic and smectic phases, while discotic tends to form columnar and nematic phases. The works involve the insertion of the calamitic side arms into the HCCP core system in order to form disk-like compounds surrounded by commonly six similar side arms of the calamitic molecules at the terminal end. To date, an enormous number of calamitic liquid crystal compounds have been synthesized and characterized. However, there are no previous works reported on synthesized compounds with hexa-arms bearing azo linking units and alkoxy terminal ends. Moreover, not many liquid crystal compounds attached to the cyclotriphosphazene core system have been studied. The main interest of this study is to understand the relationship of the skeleton structure of these types of molecules in relation to the liquid crystal mesophase. Furthermore, the synthesis of new series of azo-based cyclotriphosphazene derivatives adds into the cyclotriphosphazene molecule databases.

MATERIALS AND METHODS

1. Chemicals

The chemicals used in this study were 4-acetamidophenol, 1-bromoheptane, 1-bromononane, 1-bromodecane and 1-bromododecane, potassium iodide, potassium carbonate, sodium hydroxide, sodium nitrite, potassium hydroxide, phenol, phosphonitrilic trimer, dimethylformamide, methanol, hydrochloric acid, acetone, *n*-hexane, ethyl acetate, deuterated chloroform ($CDCl_3$), and deuterated dimethylsulphoxide (DMSO-d_6). All the chemicals were used as received without purification and these chemicals were purchased from Merck, Qrëc, Sigma-Aldrich, Across, and BDH laboratory.

2. Instruments

Fourier Transform Infrared Spectroscopy (FTIR) was used to determine the functional group present in a sample. Samples were scanned in a range of 600 to 4000 cm^{-1}. All spectra were obtained using Perkin Elmer 2000 FT-NIR Spectrometer. The molecular structures of compounds for certain atomic nuclei such as ^{1}H, ^{13}C, and ^{31}P were determined using Nuclear Magnetic Resonance Spectroscopy (NMR). The NMR spectra were obtained by using Bruker 500 MHz Ultrashield™ spectrometer. CHN analysis was accomplished by combustion analysis, in which a sample was burned in an excess of oxygen. The masses of the products of the combustion could be used to determine carbon (C), hydrogen (H), and nitrogen (N) in the sample, using a CHN analyzer, model Perkin Elmer II, 2400. Polarized Optical Microscope (POM) is a microscope with a hot stage whereby a sample is placed between two glasses on the circle slot of the hot stage. In controlled heating and cooling cycles, the liquid crystal texture of a sample can be observed. All mesophases were determined using Olympus System Mesophase BX53 linksys32.

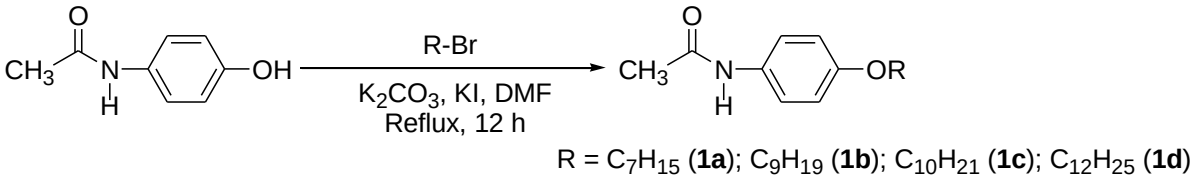

R = C_7H_{15} (**1a**); C_9H_{19} (**1b**); $C_{10}H_{21}$ (**1c**); $C_{12}H_{25}$ (**1d**)

Scheme 1. Alkylation reaction of intermediates **1a-d**

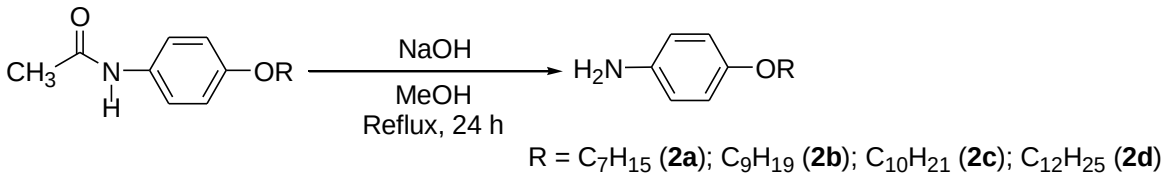

Scheme 2. Reduction reaction of intermediates **2a-d**

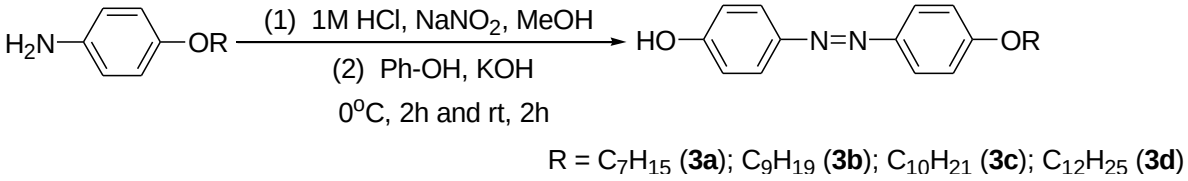

Scheme 3. Diazotization reaction of intermediates **3a-d**

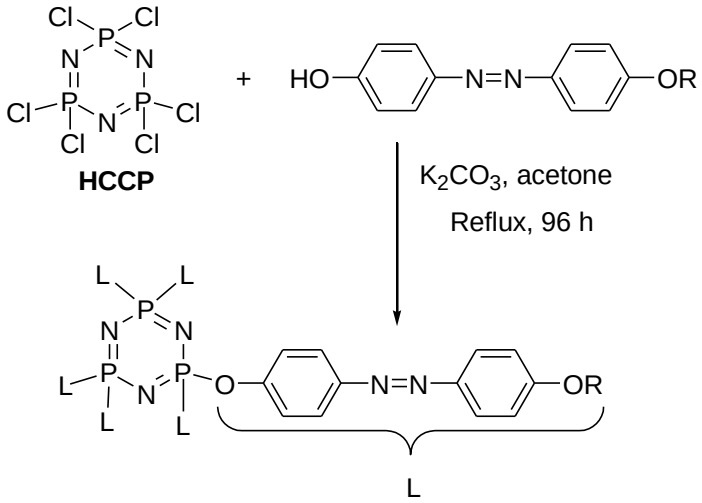

Scheme 4. Formation of hexasubstituted cyclotriphosphazene compounds **4a-d**

3. Synthesis Methods

The overall reaction pathways involved the synthesis of the series of intermediates, **1a-d**, **2a-d**, and **3a-d** (rod-like molecules), and final products, **4a-d** (disc-like molecules), are as shown in Schemes 1-4. Each reaction is discussed separately and all the synthesized products are summarized in a compact data form. The percentage yield of some intermediates and final compounds were varied, which might due to the loss of products during the filtration process.

(1a) Synthesis of *N*-(4-heptyloxyphenyl)acetamide Intermediate **1a** was synthesized according to the method reported by Barberá *et al.* (2006) with some modifications [28]. *N*-(4-hydroxyphenyl)acetamide (15.00 g, 0.099 mol) and 1-bromoheptane (17.74 g, 0.099 mol) were dissolved in 20.0 mL of DMF, separately. Both solutions were mixed together in a 250 mL round bottom flask. Potassium carbonate, K_2CO_3 (25.39 g, 0.198 mol) and potassium iodide, KI (1.64 g, 0.001 mol) were added, and the mixture was then refluxed for 12 hours. The reaction progress was monitored using TLC. Upon completion, the mixture was poured into 300 mL of cold water. Once the precipitate formed, it was filtered and dried. Recrystallization from *n*-hexane gave a light brown compound. The same method was used to synthesize **1b-d**.

Yield: 67.4%, light brown powder. FTIR (cm^{-1}): 3299 (N-H stretching), 2927 (sp^3 C-H asymmetrical stretching), 2865 (sp^3 C-H symmetrical stretching) 1654 (C=O stretching), 1515 (C=C stretching), 1244 (C-O stretching), 1162 (C-N stretching). ^{1}H-NMR (500 MHz, $CDCl_3$) δ, ppm: 7.71 (s, 1H), 7.38 (d, *J*=8.8 Hz, 2H), 6.83 (d, *J*=8.8 Hz, 2H), 3.92 (t, *J*=7.0 Hz, 2H), 2.13 (s, 1H), 1.76-1.78 (m, 2H), 1.44-1.46 (m, 2H), 1.34-1.36 (m, 6H), 0.91 (t, *J*=7.0 Hz, 3H). ^{13}C-NMR (125 MHz, $CDCl_3$) δ, ppm: 168.56, 156.02, 130.91, 122.01, 114.74, 68.32, 31.78, 29.29, 29.06, 25.99, 24.20, 22.60, 14.07. CHN elemental analysis: Calculated for $C_{15}H_{23}NO_2$: C: 72.25%, H: 9.30%, N: 5.62%; Found: C: 72.18%, H: 9.28%, N: 5.53%.

(**1b**) *N*-(4-nonyloxyphenyl)acetamide
Yield: 74.8%, beige brown powder. FTIR (cm^{-1}): 3295 (N-H stretching), 2924 (sp^3 C-H asymmetrical stretching), 2852 (sp^3 C-H symmetrical stretching) 1659 (C=O stretching), 1512 (C=C stretching), 1242 (C-O stretching), 1160 (C-N stretching). ^{1}H-NMR (500 MHz, $CDCl_3$) δ, ppm: 7.56 (s, 1H), 7.35 (d, *J*=8.9 Hz, 2H), 6.79 (d, *J*=8.9 Hz, 2H), 3.88 (t, *J*=6.5 Hz, 2H), 2.10 (s, 3H), 1.71-1.73 (m, 2H), 1.36-1.38 (m, 2H), 1.25-1.27 (m, 10H), 0.86 (t, *J*=7.0 Hz, 3H). ^{13}C-NMR (125 MHz, $CDCl_3$) δ, ppm: 168.46, 156.00, 130.93, 121.89, 114.75, 68.33, 31.87, 29.53, 29.25, 26.10, 24.27, 22.63, 14.09. CHN elemental analysis: Calculated for $C_{17}H_{27}NO_2$: C: 73.61%, H: 9.81%, N: 5.05%; Found: C: 73.47%, H: 9.95%, N: 4.98%.

(**1c**) *N*-(4-decyloxyphenyl)acetamide
Yield: 93.8%, light brown powder. FTIR (cm^{-1}): 3321 (N-H stretching), 2921 (sp^3 C-H asymmetrical stretching), 2852 (sp^3 C-H symmetrical stretching), 1662 (C=O stretching), 1508 (C=C stretching), 1242 (C-O stretching), 1159 (C-N stretching). ^{1}H-NMR (500 MHz, $CDCl_3$) δ, ppm: 7.57 (s, 1H), 7.35 (d, *J*=8.8 Hz, 2H), 6.80 (d, *J*=8.8 Hz, 2H), 3.88 (t, *J*=5.0 Hz, 2H), 2.10 (s, 3H), 1.71-1.74 (m, 2H), 1.39-1.42 (m, 2H), 1.25-1.29 (m, 12H), 0.85 (t, *J*=5.0 Hz, 3H). ^{13}C-NMR (125 MHz, $CDCl_3$) δ, ppm: 168.46, 156.00, 130.93, 121.95, 114.93, 68.32, 31.82, 29.61, 29.36, 26.03, 24.26, 22.67, 14.10. CHN elemental analysis: Calculated for $C_{18}H_{29}NO_2$: C: 74.18%, H: 10.03%, N: 4.81%; Found: C: 73.67%, H: 10.11%, N: 4.84%.

(**1d**) *N*-(4-dodecyloxyphenyl)acetamide
Yield: 86.1%, dark brown powder. FTIR (cm^{-1}): 3286 (N-H stretching), 2917 (sp^3 C-H asymmetrical stretching), 2853 (sp^3 C-H symmetrical stretching), 1655 (C=O stretching), 1506 (C=C stretching), 1241 (C-O stretching), 1164 (C-N stretching). ^{1}H-NMR (500 MHz, $CDCl_3$) δ, ppm: 7.50 (s, 1H), 7.36 (d, *J*=8.8, 2H), 6.83 (d, *J*=8.8, 2H), 3.92 (t, *J*=5.0, 2H), 2.16 (s, 3H), 1.74-1.76 (m, 2H), 1.41-1.43 (m, 2H), 1.26-1.29 (m, 18H), 0.88 (t, *J*=5.0, 3H). ^{13}C-NMR (125 MHz, $CDCl_3$) δ, ppm: 168.60, 156.00, 131.00, 121.85, 114.90, 68.30, 31.90, 29.70, 29.4, 25.80, 24.30, 22.70, 14.10. CHN elemental analysis: Calculated for $C_{20}H_{33}NO_2$: C: 75.19%, H: 10.41%, N: 4.38%; Found: C: 74.64%, H: 10.43%, N: 4.37%.

(**2a**) Synthesis of 4-heptyloxyphenylamine
Intermediate **2a** was synthesized according to the method reported by Alam *et al.* (2011) with some modifications [29]. Intermediate **1a** (8.00 g, 0.032 mol) was dissolved in 20 mL of methanol, followed by the addition of sodium hydroxide, NaOH (40.00 g, 1.000 mol) in 10 mL of water. The mixture was refluxed for 24 hours and the reaction progress was monitored using TLC. Upon completion, the mixture was poured into 200 mL of cold water and the precipitate formed was filtered and dried. Recrystallization from *n*-hexane gave a whitish powder. The same method was used to synthesize **2b-d**.

Yield: 98.6%, whitish powder. FTIR (cm^{-1}): 3390 & 3312 (N-H stretching), 2932 (sp^3 C-H asymmetrical stretching), 2868 (sp^3 C-H symmetrical stretching), 1510 (C=C stretching), 1229 (C-O stretching), 1144 (C-N stretching). ^{1}H-NMR (500 MHz, $CDCl_3$) δ, ppm: 6.77 (d, *J*=8.8, 2H), 6.66 (d, *J*=8.8 Hz, 2H), 3.90 (t, *J*=6.5 Hz, 2H), 1.75-1.77 (m, 2H), 1.45-1.47 (m, 2H), 1.34-1.37 (m, 6H), 0.92 (t, *J*=7.0, 3H). ^{13}C-NMR (125 MHz, $CDCl_3$) δ, ppm: 152.44, 139.68, 116.51, 115.71, 68.75, 31.82, 29.46, 29.11, 26.05, 22.62, 14.09. CHN elemental analysis: Calculated for $C_{13}H_{21}NO$: C: 75.32%, H: 10.21%, N: 6.76%; Found: C: 75.27%, H: 10.14%, N: 6.75%.

(**2b**) 4-Nonyloxyphenylamine
Yield: 92.1%, light brown powder. FTIR (cm^{-1}): 3392 & 3313 (N-H stretching), 2917 (sp^3 C-H asymmetrical stretching), 2852 (sp^3 C-H symmetrical stretching) 1504 (C=C stretching), 1242 (C-O stretching), 1141 (C-N stretching). ^{1}H-NMR (500 MHz, $CDCl_3$) δ, ppm: 6.72 (d, *J*=8.6 Hz, 2H), 6.61 (d, *J*=8.6 Hz, 2H), 3.86 (t, *J*=5.0, 2H), 1.71-1.73 (m, 2H), 1.40-1.42 (m, 2H), 1.27-1.30 (m, 10H), 0.87 (t, *J*=5.0, 3H). ^{13}C-NMR (125 MHz, $CDCl_3$) δ, ppm: 152.40, 139.70, 116.42, 115.70, 68.75, 31.89, 29.45, 26.08, 22.68, 14.11. CHN elemental analysis: Calculated for $C_{15}H_{25}NO$: C: 76.55%, H: 10.71%, N: 5.95%; Found: C: 76.37%, H: 10.62%, N: 5.89%.

(**2c**) 4-Decyloxyphenylamine
Yield: 68.3%, dark brown powder. FTIR (cm^{-1}): 3390 & 3315 (N-H stretching), 2920 (sp^3 C-H asymmetrical stretching), 2855 (sp^3 C-H symmetrical stretching) 1504 (C=C stretching), 1242 (C-O stretching), 1145 (C-N stretching). ^{1}H-NMR (500 MHz, $CDCl_3$) δ, ppm: 6.76 (d, *J*=8.8 Hz, 2H), 6.66 (d, *J*=8.8 Hz, 2H), 3.90 (t, *J*=10.0 Hz, 2H), 1.73-1.79 (m, 2H), 1.42-1.47 (m, 2H), 1.30-1.37 (m, 12H), 0.91 (t, *J*=5.0 Hz, 3H). ^{13}C-NMR (125 MHz, $CDCl_3$) δ, ppm: 152.40, 139.69, 116.43, 115.84, 68.75, 31.86, 29.39, 26.15, 22.68, 14.11. CHN elemental analysis: Calculated for $C_{16}H_{27}NO$: C: 77.06%, H: 10.91%, N: 5.62%; Found: C: 76.88%, H: 10.83%, N: 5.63%.

(**2d**) 4-Dodecyloxyphenylamine
Yield: 93.4%, brown powder. FTIR (cm^{-1}): 3391 & 3318 (N-H stretching), 2923 (sp^3 C-H asymmetrical stretching), 2849 (sp^3 C-H symmetrical stretching), 1514 (C=C stretching), 1238 (C-O stretching), 1140 (C-N stretching). ^{1}H-NMR (500 MHz, $CDCl_3$) δ, ppm: 6.74 (d, *J*=8.8 Hz, 2H), 6.63 (d, *J*=8.8 Hz, 2H), 3.87 (t, *J*=7.0 Hz, 2H), 1.71-1.73 (m, 2H), 1.32-1.35 (m, 18H), 0.88 (t, *J*=7.0 Hz, 3H). ^{13}C-NMR (125 MHz, $CDCl_3$) δ, ppm: 152.41, 139.67, 116.43, 115.70, 68.76, 31.92, 29.51, 26.07, 22.69, 14.11. CHN elemental analysis: Calculated for $C_{18}H_{31}NO$: C: 77.92%, H: 11.26%, N: 5.05%; Found: C: 77.68%, H: 11.23%, N: 5.01%.

(**3a**) Synthesis of 4-(4-heptyloxyphenylazo) phenol
Intermediate **3a** was synthesized according to the method reported by Sarkar *et al*. (2012) and Jamain *et al*. (2019) with some modifications [30, 31]. Intermediate **2a** (5.00 g, 0.024 mol) was mixed in 25 mL of 1 M HCl at 0°C. After 10 minutes, 10 mL of $NaNO_2$ (1.65 mol) in water was added dropwise, followed by the addition of 50 mL of methanol and the mixture was continued to stir for 30 minutes. A solution of cold phenol (2.56 mol) in 20 mL of KOH (1.34 mol) was later added dropwise for 5 minutes and the mixture was stirred at 0°C for 2 hours, followed by stirring at room temperature for another 2 more hours. The precipitate formed was filtered, washed with distilled water, and dried. Recrystallization from *n*-hexane formed a brown powder. The same method was used to synthesize **3b-d**.

Yield: 73.6%, brown powder. FTIR (cm^{-1}): 3468 & 3172 (O-H stretching), 2922 (sp^3 C-H asymmetrical stretching), 2858 (sp^3 C-H symmetrical stretching) 1602 (C=C stretching), 1472 (N=N stretching), 1239 (C-O stretching), 1152 (C-N stretching). ^{1}H-NMR (500 MHz, $CDCl_3$) δ, ppm: 7.86 (d, *J*=8.8 Hz, 2H), 7.82 (d, *J*=8.5 Hz, 2H), 6.96 (d, *J*=8.8 Hz, 2H), 6.92 (d, *J*=8.5 Hz, 2H), 4.02 (t, *J*=6.5 Hz, 2H), 1.79-1.81 (m, 2H), 1.45-1.47 (m, 2H), 1.34-1.37 (m, 6H), 0.90 (t, *J*=6.5 Hz, 3H). ^{13}C-NMR (125 MHz, $CDCl_3$) δ, ppm: 161.49, 158.38, 146.92, 146.50, 124. 79, 124.39, 115.91, 114.86, 68.50, 31.70, 29.21, 28.96, 25.94, 22.50, 13.89. CHN elemental analysis: Calculated for $C_{19}H_{24}N_2O_2$: C: 73.05%, H: 7.74%, N: 8.97%; Found: C: 72.89%, H: 7.75%, N: 8.93%.

(**3b**) 4-(4-Nonyloxyphenylazo) phenol
Yield: 67.9%, light yellow powder. FTIR (cm^{-1}): 3479-3179 (O-H stretching), 2921 (sp^3 C-H asymmetrical stretching), 2850 (sp^3 C-H symmetrical stretching) 1598 (C=C stretching), 1469 (N=N stretching), 1242 (C-O stretching), 1149 (C-N stretching). ^{1}H-NMR (500 MHz, $CDCl_3$) δ, ppm: 7.84 (d, *J*=8.5 Hz, 2H), 7.81 (d, *J*=8.3 Hz, 2H), 6.96 (d, *J*=8.5 Hz, 2H), 6.91 (d, *J*=8.3 Hz, 2H), 4.02 (t, *J*=5.0 Hz, 2H), 1.77-1.81 (m, 2H), 1.44-1.47 (m, 2H), 1.31-1.35 (m, 10H), 0.86 (t, *J*=7.1 Hz, 3H). ^{13}C-NMR (125 MHz, $CDCl_3$) δ, ppm: 161.37, 157.99, 147.25, 146.89, 124.56, 124.34, 115.80, 114.82, 68.47, 31.82, 29.46, 29.33, 29.21, 29.17, 25.99, 22.52, 13.95. CHN elemental analysis: Calculated for $C_{21}H_{28}N_2O_2$: C: 74.08%, H: 8.29%, N: 8.23%; Found: C: 73.95%, H: 8.27%, N: 8.19%.

(**3c**) 4-(4-Decyloxyphenylazo) phenol
Yield: 86.4%, light brown powder. FTIR (cm^{-1}): 3471-3178 (O-H stretching), 2920 (sp^3 C-H asymmetrical stretching), 2855 (sp^3 C-H symmetrical stretching) 1597 (C=C stretching), 1475 (N=N stretching), 1242 (C-O stretching), 1150 (C-N stretching). ^{1}H-NMR (500 MHz, $CDCl_3$) δ, ppm: 7.88 (d, *J*=8.8 Hz, 2H), 7.84 (d, *J*=8.6 Hz, 2H), 6.97 (d, *J*=8.8 Hz, 2H), 6.93 (d, *J*=8.6 Hz, 2H), 4.02 (t, *J*=5.0 Hz, 2H), 1.79-1.83 (m, 2H), 1.44-1.46 (m, 2H), 1.33-1.36 (m, 12H), 0.86 (t, *J*=6.5 Hz, 3H). ^{13}C-NMR (125 MHz, $CDCl_3$) δ, ppm: 161.59, 158.60, 146.69, 146.20, 124.96, 124.43, 115.97, 114.88, 68.50, 41.37, 29.33, 25.98, 22.56, 13.96. CHN elemental analysis: Calculated for $C_{22}H_{30}N_2O_2$: C: 74.54%, H: 8.53%, N: 7.90%; Found: C: 74.22%, H: 8.49%, N: 7.88%.

(**3d**) 4-(4-Dodecyloxyphenylazo) phenol
Yield: 85.9%, light brown powder (flakes). FTIR (cm^{-1}): 3451-3083 (O-H stretching), 2920 (sp^3 C-H asymmetrical stretching), 2850 (sp^3 C-H symmetrical stretching) 1601 (C=C stretching), 1466 (N=N stretching), 1250 (C-O stretching), 1143 (C-N stretching). ^{1}H-NMR (500 MHz, $CDCl_3$) δ, ppm: 7.83 (d, *J*=8.8 Hz, 2H), 7.79 (d, *J*=8.7 Hz, 2H), 7.04 (d, *J*=8.8 Hz, 2H), 6.95 (d, *J*=8.7 Hz, 2H), 4.00 (t, *J*=6.5 Hz, 2H), 1.76-1.80 (m, 2H), 1.45-1.47 (m, 2H), 1.26-1.29 (m, 16H), 0.86 (t, *J*=7.0 Hz, 3H). ^{13}C-NMR (125 MHz, $CDCl_3$) δ, ppm: 161.28, 159.36, 146.70, 146.61, 124.69, 124.25, 116.07, 114.79, 68.45, 31.85, 25.77, 24.11, 22.43, 22.32, 13.94. CHN elemental analysis: Calculated for $C_{24}H_{34}N_2O_2$: C: 75.35%, H: 8.96%, N: 7.32%; Found: C: 75.17%, H: 8.90%, N: 7.28%.

(**4a**) Synthesis of 4-[4'-(heptyloxyphenylazo) phenoxy]hexacyclotriphosphazene
Compound **4a** was synthesized according to the method reported by Rong *et al.* (2015) and Jamain *et al.* (2019) with some modifications [32, 33]. Intermediate **3a** (0.4342 g, 2.1 mmol), hexachlorocyclotriphophazene, CTP (0.3 mmol), and potassium carbonate, K_2CO_3 (3.6 mmol) in 80 mL of acetone were refluxed and stirred for 96 hours. The solution was cooled to room temperature and the precipitate formed was filtered, washed with water, and dried. Recrystallization from *n*-hexane gave a yellow powder. The same method was used to synthesize **4b-d**.

Yield: 68.5%, yellow powder. FTIR (cm^{-1}): 2924 (sp^3 C-H asymmetrical stretching), 2853 (sp^3 C-H symmetrical stretching), 1603 & 1583 (C=C stretching), 1493 & 1466 (N=N stretching), 1216 (C-O stretching), 1169 (P=N stretching), 980 (P-O-C stretching). ^{1}H-NMR (500 MHz, DMSO-d_6) δ, ppm: 7.73 (d, *J*=8.8 Hz, 2H), 7.62 (d, *J*=8.5 Hz, 2H), 6.99 (d, *J*=8.8 Hz, 2H), 6.76 (d, *J*=8.5 Hz, 2H), 4.09 (t, *J*=6.5 Hz, 2H), 1.73-1.75 (m, 2H), 1.40-1.42 (m, 2H), 1.24-1.27 (m, 6H), 0.85 (t, J=7.0 Hz, 3H). ^{13}C-NMR (125 MHz, DMSO-d_6) δ, ppm: 160.54, 159.95, 146.42, 145.51, 123.80, 123.48, 115.66, 114.93, 68.08, 30.51, 28.08, 27.63, 24.77, 21.24, 12.98. ^{31}P-NMR (DMSO-d_6) δ, ppm: 9.73. CHN elemental analysis: Calculated for $C_{114}H_{138}N_{15}O_{12}P_3$: C: 68.35%, H: 6.94%, N: 10.49%; Found: C: 68.27%, H: 6.90%, N: 10.45%.

(**4b**) 4-[4'-(Nonyloxyphenylazo)phenoxy]hexacyclotriphosphazene
Yield: 89.4%, dark brown powder. FTIR (cm^{-1}): 2927 (sp^3 C-H asymmetrical stretching), 2853 (sp^3 C-H symmetrical stretching), 1609 & 1584 (C=C

stretching), 1496 & 1471 (N=N stretching), 1214 (C-O stretching), 1170 (P=N stretching), 958 (P-O-C stretching). ^{1}H-NMR (500 MHz, DMSO-d_6) δ, ppm: 7.76 (d, *J*=8.5 Hz, 2H), 7.69 (d, *J*=8.3 Hz, 2H), 7.09 (d, *J*=8.5 Hz, 2H), 6.88 (d, *J*=8.3 Hz, 2H), 4.01 (t, *J*=5.0 Hz, 2H), 1.78-1.80 (m, 2H), 1.45-1.47 (m, 2H), 1.29-1.33 (m, 12H), 0.87 (t, *J*=7.0 Hz, 3H). ^{13}C-NMR (125 MHz, DMSO-d_6) δ, ppm: 161.69, 151.82, 150.16, 146.99, 124.76, 123.85, 121.39, 114.71, 68.46, 31.73, 29.62, 29.29, 29.01, 25.99, 22.51, 13.88. ^{31}P-NMR (DMSO-d_6) δ, ppm: 9.72. CHN elemental analysis: Calculated for $C_{126}H_{162}N_{15}O_{12}P_3$: C: 69.69%, H: 7.52%, N: 9.67%; Found: C: 69.47%, H: 7.48%, N: 9.63%.

(**4c**) 4-[4'-(Decyloxyphenylazo)phenoxy]hexacyclotriphosphazene
Yield: 73.5%, light yellow powder. FTIR (cm^{-1}): 2923 (sp^3 C-H asymmetrical stretching), 2855 (sp^3 C-H symmetrical stretching), 1605 & 1582 (C=C stretching), 1493 & 1467 (N=N stretching), 1216 (C-O stretching), 1163 (P=N stretching), 963 (P-O-C stretching). ^{1}H-NMR (500 MHz, DMSO-d_6) δ, ppm: 7.74 (d, *J*=8.8 Hz, 2H), 7.69 (d, *J*=8.6 Hz, 2H), 7.03 (d, *J*=8.8 Hz, 2H), 6.93 (d, *J*=8.6 Hz, 2H), 4.05 (t, *J*=6.6 Hz, 2H), 1.70-1.75 (m, 2H), 1.40-1.45 (m, 2H) 1.24-1.34 (m, 2H), 0.84 (t, *J*=6.5 Hz, 3H). ^{13}C-NMR (125 MHz, DMSO-d_6) δ, ppm: 160.55, 159.97, 146.42, 145.50, 123.80, 123.49, 115.68, 114.92, 68.07, 30.85, 28.52-28.18, 28.18, 25.07, 21.56, 13.28. ^{31}P-NMR (DMSO-d_6) δ, ppm: 9.73. CHN elemental analysis: Calculated for $C_{132}H_{174}N_{15}O_{12}P_3$: C: 70.28%, H: 7.77%, N: 9.31%; Found: C: 70.25%, H: 7.77%, N: 9.30%.

(**4d**) 4-[4'-(Dodecyloxyphenylazo)phenoxy]hexacyclotriphosphazene
Yield: 78.8%, yellow powder. FTIR (cm^{-1}): 2925 (sp^3 C-H asymmetrical stretching), 2852 (sp^3 C-H symmetrical stretching), 1602 & 1582 (C=C stretching), 1493 & 1466 (N=N stretching), 1217 (C-O stretching), 1169 (P=N stretching), 980 (P-O-C stretching). ^{1}H-NMR (500 MHz, DMSO-d_6) δ, ppm: 7.70 (d, *J*=8.8 Hz, 2H), 7.60 (d, *J*=8.7 Hz, 2H), 7.02 (d, *J*=8.8 Hz, 2H), 6.72 (d, *J*=8.7 Hz, 2H), 4.06 (t, *J*=6.50 Hz, 2H), 1.74-1.76 (m, 2H), 1.42-1.45 (m, 2H), 1.28-1.34 (m, 16H), 0.86 (t, *J*=7.0 Hz, 3H). ^{13}C-NMR (125 MHz, DMSO-d_6) δ, ppm: 162.33, 151.17, 150.63, 146.87, 123.96, 123.00, 114.92, 113.63, 68.66, 30.78, 28.38-28.21, 28.09, 25.04, 21.47, 13.16. ^{31}P-NMR (DMSO-d_6) δ, ppm: 9.72. CHN elemental analysis: Calculated for $C_{144}H_{198}N_{15}O_{12}P_3$: C: 71.35%, H: 8.23%, N: 8.67%; Found: C: 71.25%, H: 8.20%, N: 8.63%.

RESULTS AND DISCUSSION

1. FTIR Spectral Discussion

Acetamidophenol is a common starting material used as it is cheap and easily obtainable. The alkylation reaction of acetamidophenol with a series of alkyl halides yielded the alkylated products, **1a-d**.

Intermediate **1c** is used as the representative compound. The absorption band for **1c** in Figure 2 shows the presence of the N-H stretching at 3321 cm^{-1} which confirms the secondary amine. The absorption bands at 2921 and 2852 cm^{-1} refer to the C-H (sp^3) asymmetrical and symmetrical stretching. Other absorption bands are the C=O stretch at 1662 cm^{-1}, the aromatic C=C stretch at 1508, C-O stretch at 1242 cm^{-1}, and C-N stretch at 1159 cm^{-1}.

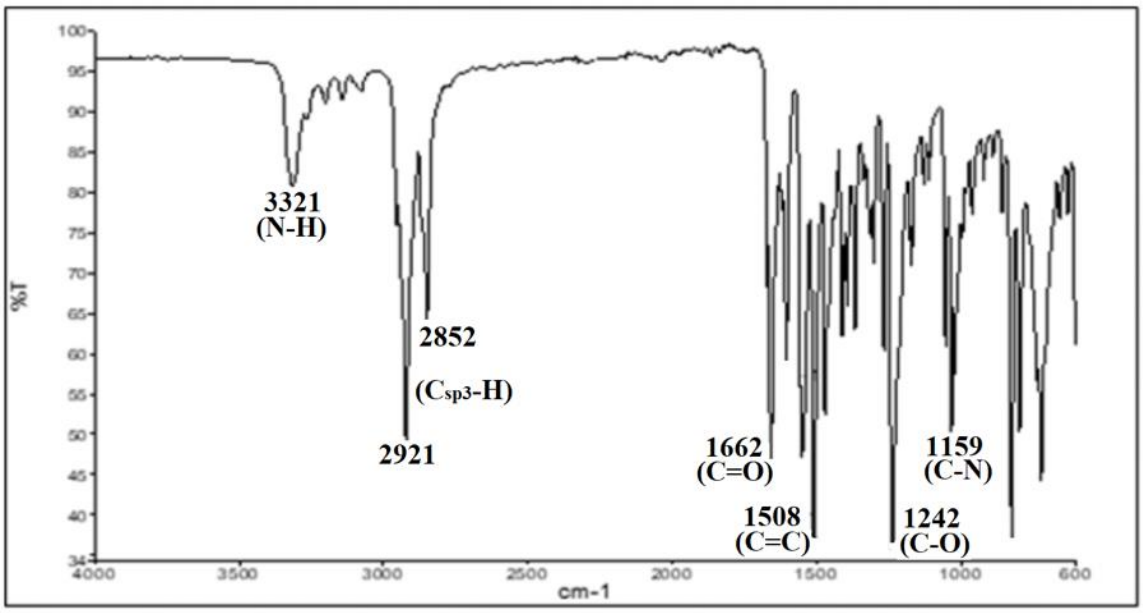

Figure 2. The FTIR spectrum of **1c**

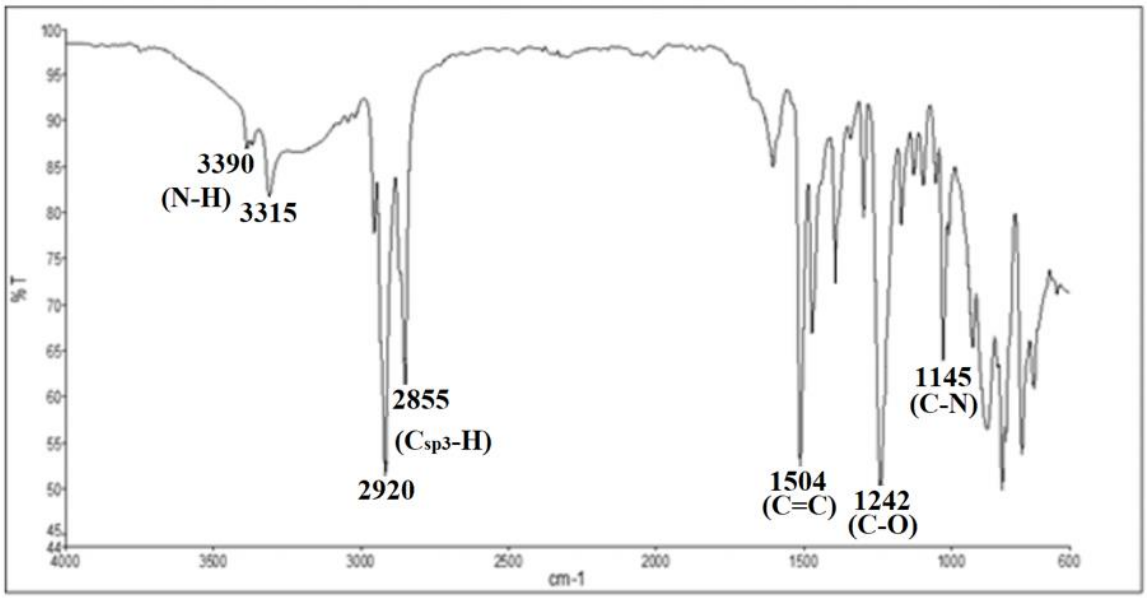

Figure 3. The FTIR spectrum of **2c**

The reduction reaction of intermediates **1a-d** gave the corresponding intermediates **2a-d** with the amino group at the para position of the benzene ring. Intermediate **2c** is used as the representative compound. Figure 3 shows the FTIR spectrum of **2c** in which two absorption bands at 3390 and 3315 cm^{-1} correspond to the primary amines in the amino group. Two side by side absorption bands at 2920 and 2855 cm^{-1} refer to the C-H (sp^3) asymmetrical and symmetrical stretching. Other absorptions include the band at 1504 cm^{-1} for the aromatic C=C stretching, 1242 cm^{-1} for the C-O stretching, and 1145 cm^{-1} for the C-N stretching. The disappearance of the absorption band in the region of 1700-1650 cm^{-1} for C=O shows that the reaction was successful.

The diazotization reaction of **2a-d** with nitrous acid, followed by the addition of cold phenol in KOH solution gave a series of compounds **3a-d**. Intermediate **3c** is used as the representative compound. Figure 4 shows a broad absorption band in the FTIR spectrum of **3c** in the range of 3178-3471 cm^{-1}, which corresponds to the O-H stretching. The side by side bands at 2920 and 2855 cm^{-1} refer to the C-H (sp^3) asymmetrical and symmetrical stretching, respectively. Other absorptions include the band at 1597 cm^{-1} for the C=C stretching and 1475 cm^{-1} for the N=N stretching, which confirm the successful formation of the azo group in this reaction. Absorptions bands at 1242 and 1150 cm^{-1} refer to the C-O and C-N stretching, respectively.

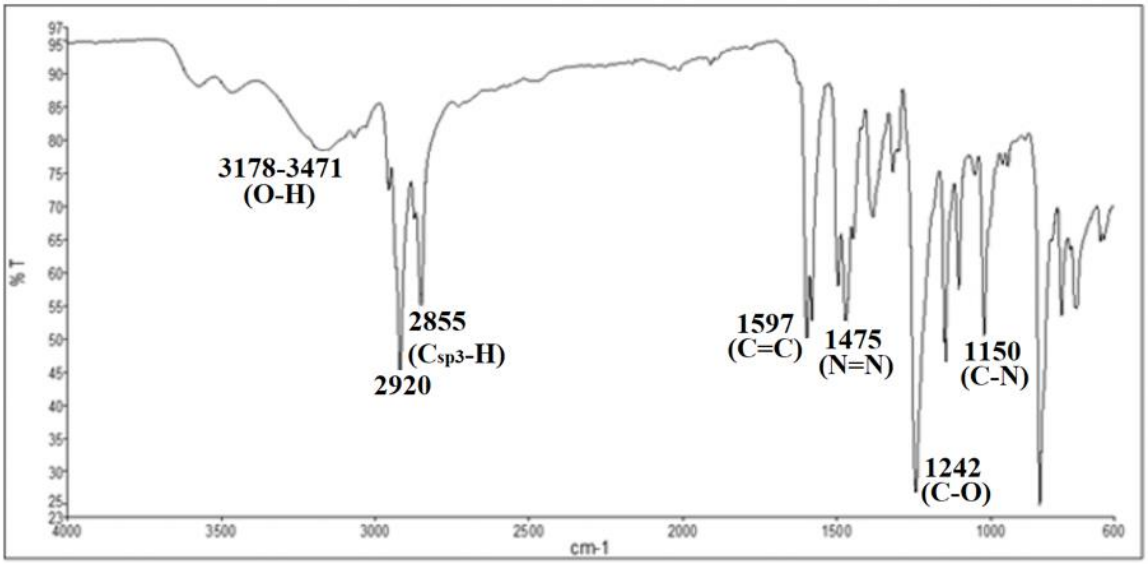

Figure 4. The FTIR spectrum of **3c**

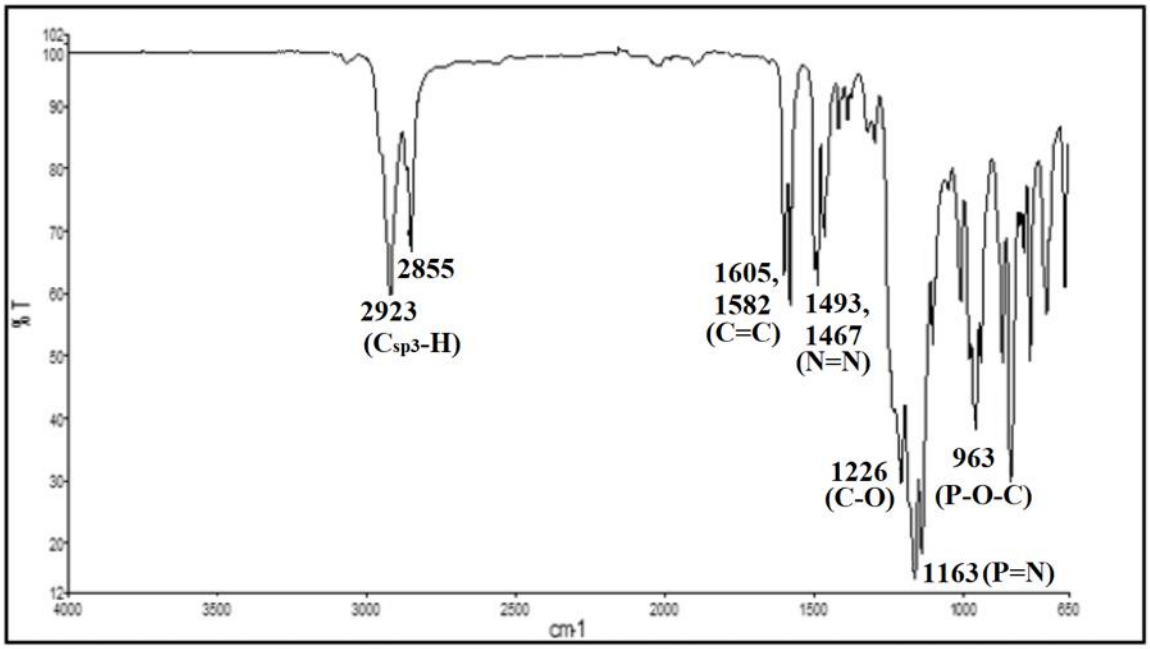

Figure 5. The IR spectrum of **4c**

Table 1. FTIR data of **1a–d**, **2a-d**, **3a-d**, and **4a–d**

Cpd	Vibrational (stretching, cm^{-1})									
	N-H (amide)	**N-H (amino)**	**O-H**	**C-H (sp3)**	**C=O**	**C=C**	**N=N**	**C-O**	**P=N**	**C-N**
1a	3299	-	-	2927, 2865	1654	1515	-	1240	-	1162
1b	3295	-	-	2924, 2852	1659	1512	-	1243	-	1160
1c	3321	-	-	2921, 2852	1662	1508	-	1242	-	1159
1d	3286	-	-	2917, 2853	1655	1506	-	1241	-	1164
2a	-	3390, 3312	-	2932, 2868	-	1510	-	1229	-	1144
2b	-	3392, 3313	-	2917, 2852	-	1504	-	1242	-	1141
2c	-	3390, 3315	-	2920, 2855	-	1514	-	1242	-	1145
2d	-	3391, 3318	-	2923, 2849	-	1514	-	1238	-	1140
3a	-	-	3468-3172	2922, 2858	-	1602	1472	1239	-	1152
3b	-	-	3479-3179	2921, 2850	-	1598	1469	1242	-	1149
3c	-	-	3471-3178	2920, 2855	-	1597	1475	1242	-	1150
3d	-	-	3451-3083	2920, 2850	-	1601	1466	1250	-	1143
4a	-	-	-	2924, 2853	-	1603, 1583	1493, 1466	1216	1169	-
4b	-	-	-	2927, 2853	-	1609, 1584	1496, 1471	1214	1170	-
4c	-	-	-	2923, 2855	-	1605, 1582	1493, 1467	1216	1163	-
4d	-	-	-	2925, 2852	-	1602, 1582	1493, 1466	1217	1169	-

Note: Cpd = Compound

The substitution reaction of the hexachlorocyclotriphosphazene with the rod-like intermediates having the azo group, **3a-d** formed a series of discotic molecules, **4a-d**. Compound **4c** is used as the representative compound. Figure 5 shows the IR spectrum of **4c** in which two absorption bands at 2923 and 2855 cm^{-1} refer to the C-H (sp^3) asymmetrical and symmetrical stretching. No broad absorption of the O-H stretching in the region of 3100-3300 cm^{-1} confirms that the intermediates have been successfully substituted for the cyclotriphosphazene core. The absorption bands at 1605 and 1582 cm^{-1} refer to the aromatic C=C stretching while the absorption bands at 1493 and 1467 cm^{-1} refer to the N=N stretching of the azo group. Other absorption bands at 1226 and 1163 cm^{-1} indicate the C-O and P=N stretching, respectively. Meanwhile, the band at 963 cm^{-1} refers to the P-O-C stretching. The overall FTIR data of **1a–d**, **2a-d**, **3a-d**, and **4a–d** are summarized in Table 1.

2. NMR Spectral Discussion

The ^{1}H, ^{13}C, and ^{31}P-NMR data for the intermediates and final compounds are summarized in a compact data form. Intermediates **1a-d** revealed the same pattern and intermediate **1c** is used as a representative for the other intermediates. In the ^{1}H-NMR spectrum (Figure 1a), a singlet at δ 7.57 ppm is assigned for the amide proton. Two doublets at δ 6.80 and 7.35 ppm are the aromatic protons, while the peaks for the aliphatic chain are observed as a triplet at δ 3.88, multiplets at 1.71-1.74, 1.39-1.42, and 1.25-1.29, and a triplet at δ 0.85 ppm. The methyl protons are assigned to a singlet at δ 2.10 ppm. The ^{13}C-NMR spectrum (Figure 1b) shows a carbonyl amide carbon at δ 168.46 ppm. The peaks for the aromatic carbons are observed in the region of δ 114.74-156.00 ppm, and the aliphatic chains show the peak in the region of δ 14.10-68.32 ppm. The presence of aliphatic protons in **1a-d** indicated that the alkylation reaction was successful.

Intermediates **2a-d** were formed from the reduction of **1a-d**. The amide proton was not observed in **2a-d**, which confirmed the reduction reaction was a success. Intermediate **2c** is used as a representative compound. The ^{1}H-NMR spectrum of **2c** (Figure 7a) shows two doublets at δ 6.66 and 6.76 ppm, and the aliphatic protons as a triplet at δ 3.90, multiplets at δ 1.73-1.79, 1.42-1.47, and 1.30-1.37, and a triplet at δ 0.91 ppm. The ^{13}C-NMR spectrum of **2c** (Figure 7b) shows the aromatic carbons in the region of δ 115.70-152.40 ppm and the aliphatic carbons in the region of δ 14.11-68.75 ppm.

The diazotization reaction between **2a-d** with phenol formed intermediates **3a-d**. Azo intermediate **3c** has two benzene rings. The ^{1}H-NMR spectrum of the representative compound **3c** (Figure 8a) shows four doublets at δ 6.93, 6.97, 7.84, and 7.88 ppm, and the aliphatic protons as a triplet at δ 4.02 ppm, multiplets at δ 1.79-1.83, 1.44-1.46, and 1.33-1.36 ppm, and a triplet at δ 0.86 ppm. The ^{13}C-NMR spectrum of **3c** (Figure 8b) shows the aromatic carbons in the region of δ 114.88-161.56 ppm and the aliphatic carbons in the region of δ 13.96-68.50 ppm.

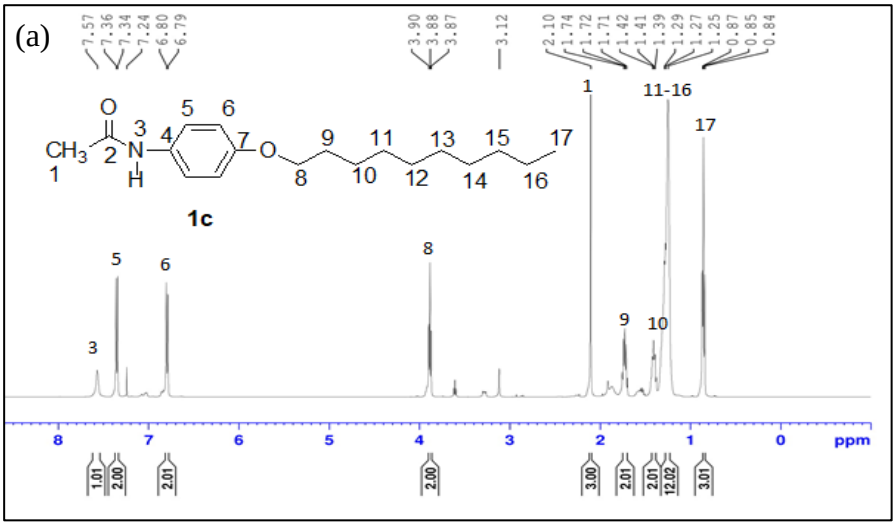

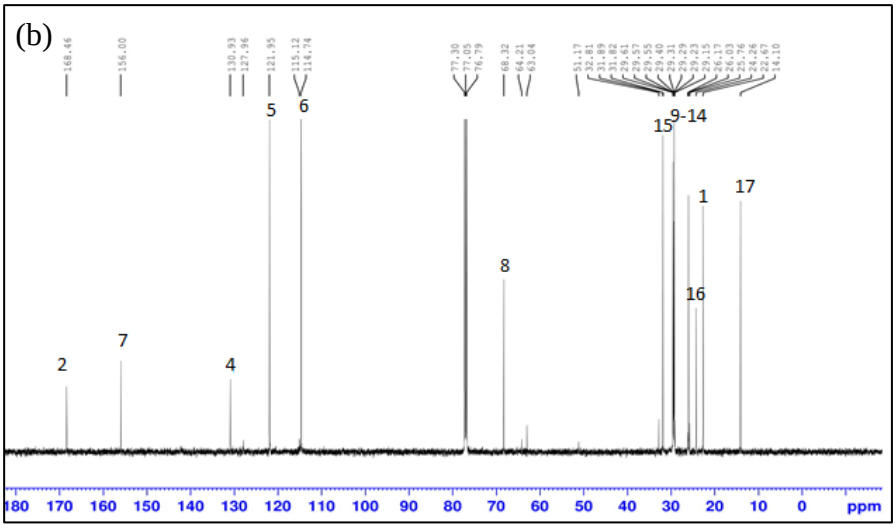

Figure 6. (a) ^{1}H-NMR (500 MHz, $CDCl_3$) and (b) ^{13}C-NMR (125MHz, $CDCl_3$) spectra of intermediate **1c**

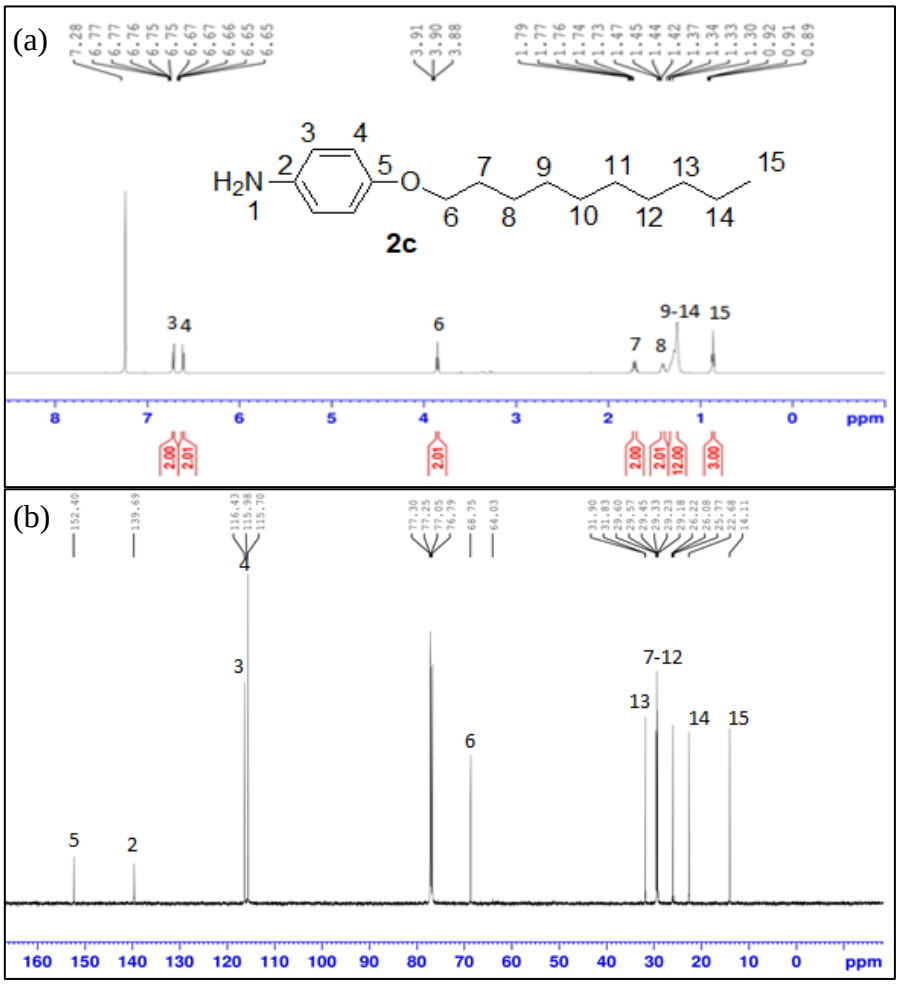

Figure 7. (a) ^{1}H-NMR (500 MHz, $CDCl_3$) and (b) ^{13}C-NMR (125MHz, $CDCl_3$) spectra of intermediate **2c**

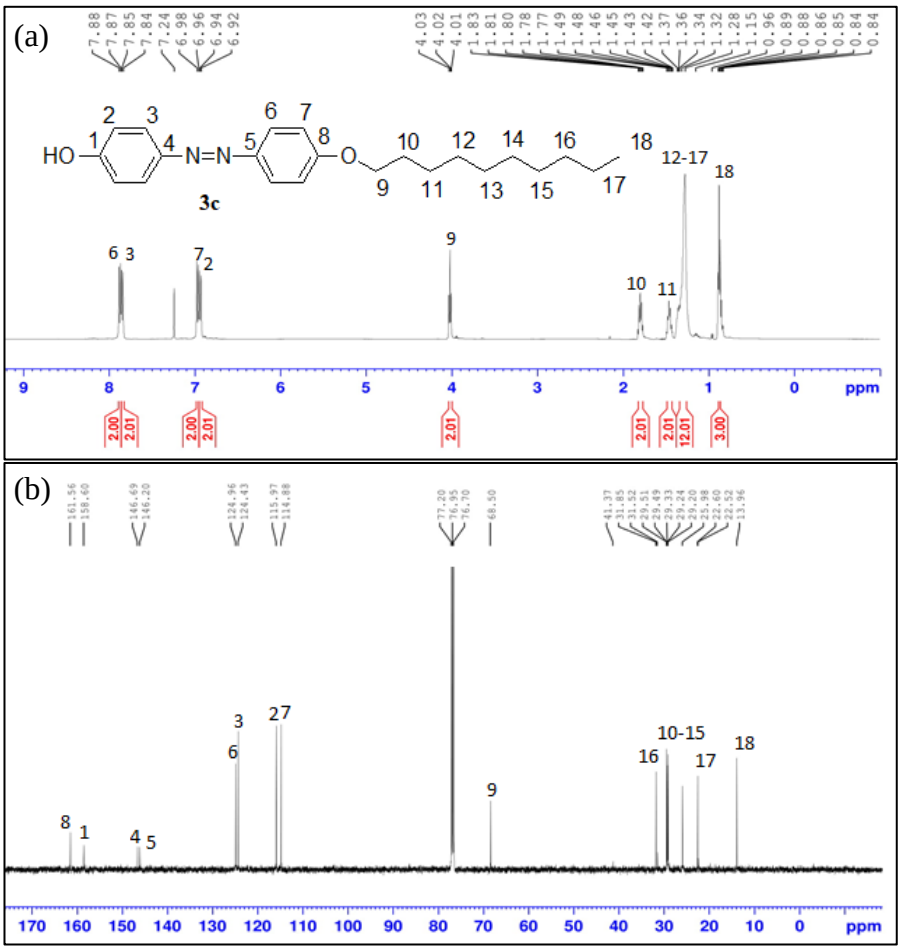

Figure 8. (a) ^{1}H-NMR (500 MHz, $CDCl_3$) and (b) ^{13}C-NMR (125MHz, $CDCl_3$) spectra of intermediate **3c**

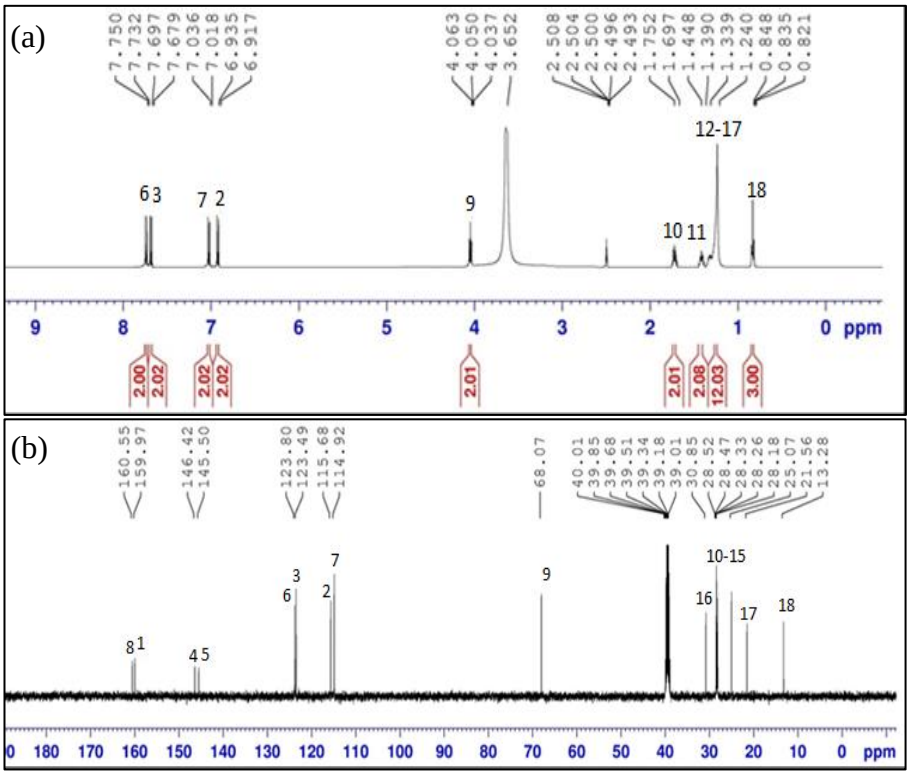

Figure 9. (a) ^{1}H-NMR (500 MHz, DMSO-d_6) and (b) ^{13}C-NMR (125MHz, DMSO-d_6) spectra of compound **4c**

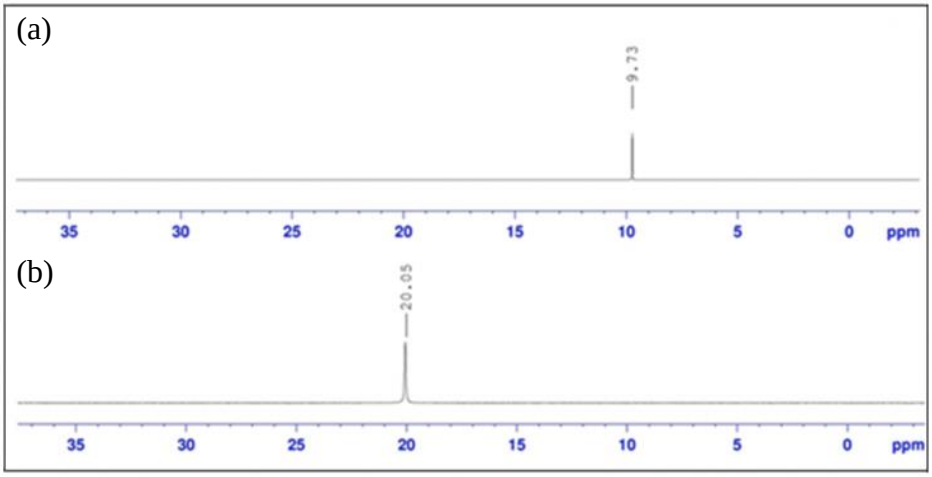

Figure 10. ^{31}P-NMR spectra (500 MHz, DMSO-d_6) of (a) compound **4c** and (b) **HCCP**

Table 2. The chemical shifts (^{1}H, ^{13}C, and ^{31}P) of compounds **4a-d**

Compound	Chemical Shift (ppm)				
	^{1}H		^{13}C		^{31}P
	Aromatic-H	Aliphatic-H	Aromatic-C	Aliphatic-C	Hexa-P
4a	7.73 (d), 7.62 (d), 6.99 (d), 6.76 (d)	4.09 (t), 1.73-1.75 (m), 1.40-1.42 (m), 1.24-1.27 (m), 0.85 (t)	160.54, 159.95, 146.42, 145.51, 123.80, 123.48, 115.66, 114.93	68.08, 30.51, 28.08, 27.63, 24.77, 21.24, 12.98	9.73
4b	7.76 (d), 7.69 (d), 7.09 (d), 6.88 (d)	4.01 (t), 1.78-1.80 (m), 1.45-1.47 (m), 1.29-1.33 (m), 0.87 (t)	161.69, 151.82, 150.16, 146.99, 124.76, 123.85, 121.39, 114.71	68.46, 31.73, 29.62, 29.29, 29.01, 25.99, 22.51, 13.88	9.72
4c	7.74 (d), 7.69 (d), 7.03 (d), 6.93 (d)	4.05 (t), 1.70-1.75 (m), 1.40-1.45 (m) 1.24-1.34 (m), 0.84 (t)	160.55, 159.97, 146.42, 145.50, 123.80, 123.49, 115.68, 114.92	68.07, 30.85, 28.52-28.18, 28.18, 25.07, 21.56,13.28	9.73
4d	7.70 (d), 7.60 (d), 7.02 (d), 6.72 (d)	4.06 (t), 1.74-1.76 (m), 1.42-1.45 (m), 1.28-1.34 (m), 0.86 (t)	162.33, 151.17, 150.63, 146.87, 123.96, 123.00, 114.92, 113.63	68.66, 30.78, 28.38-28.21, 28.09, 25.04, 21.47, 13.16	9.72

The substitution reaction of rod-like intermediates **3a-d** formed discotic compounds **4a-d**. Using **4c** as a representative compound, the reaction was considered successful. In the ^{1}H-NMR spectrum of **4c** (Figure 9a) there are four doublets at δ 6.93, 7.03, 7.69, and 7.74 ppm, and the aliphatic protons as a triplet at δ 4.05 ppm, multiplets at δ 1.70-1.75, 1.40-1.45, and 1.24-1.34 ppm, and a triplet at δ 0.84 ppm. The ^{13}C-NMR spectrum of **4c** (Figure 9b) shows the aromatic carbons in the region of δ 114.92-160.55 ppm and the aliphatic carbons in the region of δ 12.98-68.08 ppm. Meanwhile, the ^{31}P-NMR spectrum (Figure 10a) of compound **4c** shows only a singlet at δ 9.73 ppm, which indicates that all the phosphorus

have been substituted with the same side arms. The ^{31}P-NMR spectrum of compound **4c** experienced more shielding compared to that of **HCCP,** as shown in Figure 10b (20.05 ppm), which has six electron withdrawing chlorine atoms. This was due to high electron density of the hexa-series that contain six chlorine side arms [15]. As a result, greater shielding effect was observed. The chemical shifts (^{1}H, ^{13}C, and ^{31}P) for compounds **4a-d** are summarized in Table 2.

3. Determination of Mesophase Behaviour using POM

POM is a common microscopy technique to detect the liquid crystal phases. The sample which is placed under the microscope with controlled temperature exhibits textures of the phase changes. The synthesis of LC molecules requires at least two aromatic rings, either cycloaliphatic or a combination of one aromatic and one cycloaliphatic ring, which are connected directly or through a suitable linking unit. In this work, all the rod-like intermediates, **3a-d** and the disc-like compounds, **4a-d** were tested for liquid crystal properties. All the data are summarized in Table 3. Unfortunately, all the synthesized compounds were found to be non-mesogenic without liquid crystal properties.

In general, the skeleton structures of a molecule influence the liquid crystal properties. A compound must possess certain requirements in order to exhibit liquid crystal mesophase [33]. The physical properties of even the simplest liquid crystal compound are truly remarkable due to the self-assembly of molecules in an ordered, yet fluid, liquid crystal mesophase [34]. The main criteria for a molecule to adopt liquid crystal behaviour include the molecular shape which should be relatively thin or flat within rigid molecular frameworks, which usually based on benzene rings [31, 35]. The structure should not be branched or angular (bilateral substitution), which might disrupt the linearity of the molecule.

Table 3. POM data for mesophase transitions of **3a-d** and **4a-d**

Shape of Compound	Compound	Mode	Transition Temperature
Rod-like	**3a**	Heating	Cr → I 102.0 °C
		Cooling	I → Cr 88.0 °C
	3b	Heating	Cr → I 103.0 °C
		Cooling	I → Cr 98.4 °C
	3c	Heating	Cr → I 108.6 °C
		Cooling	I → Cr 102.9 °C
	3d	Heating	Cr → I 111.6 °C
		Cooling	I → Cr 104.9 °C
Disc-like	**4a**	Heating	Cr → I 122.5 °C
		Cooling	I → Cr 110.3 °C
	4b	Heating	Cr → I 123.8 °C
		Cooling	I → Cr 111.3 °C
	4c	Heating	Cr → I 125.6 °C
		Cooling	I → Cr 108.1 °C
	4d	Heating	Cr → I 127.8 °C
		Cooling	I → Cr 109.5 °C

Rod-shaped molecules have an elongated, anisotropic geometry, which is maintained through the rigidity and linearity of its constituents. In liquid crystal molecules, linking units connect one core to another and are also used to link the terminal chain to the core. The more polar linking units have higher viscosity. In this research, azo linking units were used to increase the molecular length and maintain the rigidity of the molecules [31]. These groups conjugated with aromatic rings and were able to enhance the anisotropic polarizability [36]. Azo linking units provided linearity to the rod-like structure of the molecules, which allowed them to adopt liquid crystal properties. Aromatic ring cores connected directly or through linking units were very useful in providing rigidity to the molecules [37]. The ring system affected the liquid crystal stability and other physical properties, allowing linear configuration.

Terminal substituents can both attract and repel one another in different molecules. They can also affect the polarizability of the aromatic rings to which they are attached [38, 39]. In addition, terminal substituents may interact with the lateral portion of an adjacent molecule. It was reported that alkyl side chain length had also been demonstrated to have a dramatic effect on mesophase formation [15, 40]. Increased aliphatic side chains led to greater organization in the liquid phase, which in turn gives wider liquid crystal mesophases [41, 42]. In contrast, intermediates **3a-d** attached with the hydroxy and alkyl terminal groups did not exhibit any liquid crystal behavior. The presence of the hydroxy group led to the cancellation of the dipole moment in the molecules. Previous research showed that the presence of azo linking units bearing nitro and alkyl terminal groups induce the formation of the smectic phases [43]. This phenomenon is attributed by the presence of the nitro substituent as an electron withdrawing group. This group is able to maximize the repulsive interactions between adjacent aromatic π-systems and then induces the mesophase transition [15, 44].

However, the introduction of non-mesogenic intermediate side arms will eventually give non-mesogenic products. POM analysis proved that the insertion of the rod-like intermediates, **3a-d** without any liquid crystal behavior produced non-mesogenic compounds, **4a-d**. This phenomenon was due to the decrease of the ring flexibility of the calamitic side arms, which was caused by the length of the terminal chain and affected the transition temperature [45, 46]. The presence of the phosphazene core system caused the average clearing temperature to increase. This behavior was attributed to the larger core size, which directly impacts the π-stacking. It can be concluded that the clearing temperature for intermediates **3a-d** and compounds **4a-d** was increased with the increasing of the chain length at the terminal chain. Unfortunately, the elongated structure of the azo molecule still did not exhibit any liquid crystal phase.

The cancellation of dipole moments of the molecules might occur as the delocalization of the lone pair of electrons or π bonds in the azo linking unit tend to resonate onto the aromatic ring. As a result, the benzene ring deactivated and the molecular interactions needed for the formation of mesophases could not be induced.

CONCLUSION

All the intermediates (**1a-d**, **2a-d**, and **3a-d**) and discotic compounds with the azo linking units, **4a-d** with different terminal chain lengths were successfully synthesized and characterized. All these intermediates and final compounds were characterized by using FTIR, ^{1}H and ^{13}C-NMR, and CHN elemental analysis. The existence of azo linkage in the FTIR spectroscopy study confirmed the successful synthesis of the final compounds. The POM observation showed that all the intermediates and compounds were non-mesogenic without liquid crystal behavior. Even though the azo linkage provided a linearity to the structure, the presence of non-mesogenic intermediate side arms in the HCCP core system would produce non-mesogenic products. In the heating cycle, the clearing temperature of compounds **4a-d** were observed at 122.5, 123.8, 125.6, and 127.8°C, respectively.

ACKNOWLEDGEMENT

The authors would like to thank the Universiti Malaysia Sabah (UMS) for Grant No. SGA0037-2019 and Universiti Sains Malaysia (USM) for RUI (USM) Grant No. 1001/PKIMIA/811332.

REFERENCES

1. Andrienko, D. (2018) Introduction to liquid crystals, *J. Mol. Liq.*, **267**, 520–541.

2. Reinitzer, F. (1989) Contributions to the knowlegde of cholesterol. *Liq. Cryst.*, **5**, 7–18. Translation of Reinitzer (1888).

3. Hird, M., Goodby, J. W., Gough, N., Toyne, K. J. (2001) Novel liquid crystals with a bent molecular shape containing a 1,5-disubstituted 2,3,4-trifluorophenyl unit. Banana-shaped liquid crystals-synthesis and properties, *J. Mater. Chem.*, **11**, 2732–2742.

4. Takashi, K., Yuki, H., Suguru, N., Masaya, M. (2007) Liquid-crystalline physical gels, *Chem. Soc. Rev.*, **36(12)**,1857–1867.

5. Collings, P. J., Hird, M. (1998) Introduction to Liquid Crystals: Chemistry and Physics, *Taylor and Francis, MIT Press*, **210**.

6. Allcock, H. R. (1972) Phosphorus-Nitrogen Compounds; *Academic Press: New York*.

7. Allcock, H. R. (1972) Recent advances in phosphazene (phosphonitrilic) chemistry, *Chem. Rev.*, **72(4)**, 315–356.

8. Rong, Y., Bo, W., Xiaofeng, H., Binbin, M., Jinchun, L. (2017) Synthesis and characterization of flame retardant rigid polyurethane foam based on a reactive flame retardant containing phosphazene and cyclotriphosphazene, *Polym. Degrad. Stab.*, **144**, 62–69.

9. Barberá, J., Bardají, M., Jiménez, J., Laguna, A., Martínez, M. P., Oriol, L., Zaragozano, I. (2005) Columnar mesomorphic organizations in cyclotriphosphazenes, *J. Am. Chem. Soc.*, **127(25)**, 8994–9002.

10. Zhu, L., Zhu, Y., Pan, Y., Huang, Y. W., Huang, X. B., Tang, X. Z. (2007) Fully cross-liked poly[-cyclotriphosphazene-co-(4,40-sulfonyldiphenol)] microspheres via precipitation polymerization and their superior thermal properties, *Macromol. React. Eng.*, **1**, 45–52.

11. Lejeune, N., Dez, I., Jaffres, P. A., Lohier, J. F., Madec, P. J., Santos, J. S. O. (2008) Synthesis, crystal structure and thermal properties of phosphorylated cyclotriphosphazenes, *Eur. J. Inorg. Chem.*, **1**, 138–143.

12. Allcock, H. R. (2004) The crucial role of inorganic ring chemistry in the development of new polymers, *Phosphorus, Sulfur Silicon Relat. Elem.*, **179(4-5)**, 661–671.

13. Pan, Y., Wang, C. (2020) Periodic oscillation of the optical trasmittance in azo dye-doped liquid crystal between two crossed polarizers. *Opt. Commun.*, **461**, 125225.

14. Hamdi, R., Khalfallah, C. B., Soltani, T. (2020). Synthesis and study of physicochemical properties of relatively high birefringence liquid crystals: Tolane-type with symmetric alkoxy side groups. *J. Mol. Liq.*, **310**, 113205.

15. Jamain, Z., Khairuddean, M., Guan-Seng, T. (2020) Liquid-crystal and fire-retardant properties of new hexasubstituted cyclotriphosphazene compounds with two Schiff base linking units. *Molecules*, **25**, 2122.

16. Allcock, H. R., Klingenberg, E. H. (1995) Synthesis of liquid crystalline phosphazenes containing chiral mesogens. *Macromolecules*, **28**, 4351–4360.

17. Ichimura, K. (2000) Photoalignment of liquid crystal systems, *Chem. Rev.*, **100**, 1847–1873.

18. Ikeda, T. (2003) Photomodulation of liquid crystal orientations for photonic applications, *J. Mater. Chem.*, **13**, 2037–2057.

19. Allcock, H. R., Kim, C. (1989) Liquid crystalline phosphazenes. High polymeric and cyclic trimeric systems with aromatic azo side groups, *Macromolecules*, **22**, 2596–2602.

20. Allcock, H. R. (2003) Chemistry and Applications of Polyphosphazenes, *Wiley Interscience, New York*.

21. Savvilotidou, V., Kousaiti, A., Batinic, B., Vaccari, M., Kastanaki, E., Karagianni, K., Gidarakos, E. (2019) Evaluation and comparison of pre-treatment techniques for recovering indium from discarded liquid crystal displays. *Waste Manage.*, **87**, 51–61.

22. Xinfang, Z., Raheel, A., Shuangkun, Z., Hanlin, M., Zhanpeng, W., Dezhen, W. (2017) Hexa(eugenol)cyclotriphosphazene modified bismaleimide resins with unique thermal stability and flame retardancy, *React. Funct. Polym.*, **113**, 77–84.

23. Michal, D., Marcin, P., Rafal, J., Hieronim, M. (2018) Synthesis and flame retardant efficacy of hexakis(3-(triethoxysilyl)propyloxy)cyclotri-phosphazene/silica coatings for cotton fabrics, *Polym. Degrad. Stab.*, **148**, 10–18.

24. Jaeger, R. D., Gleria, M. (1998) Poly (organophosphazene)s and related compounds; synthesis properties and application, *Progr. Poym. Sci.*, **23(2)**, 179–276.

25. Arines, J. (2009) Impact of liquid crystals in active and adaptive optics, *Materials*, **2(2)**, 549–561.

26. Şenkuytu, E., Kızılkaya, P., Ölçer, Z., Pala, Davarcı, U., D., Zorlu, Y., Erdoğan, H., Çiftçi, G. Y. (2020) Electrophoresis and biosensor-based DNA interaction analysis of the first paraben derivatives of spermine-bridged cyclo-triphosphazenes. *Inorg. Chem.*, **59**, 2288-2298.

27. Iqbal, D., Samiullah, M. S. (2013) Photo-responsive shape-memory and shape-changing liquid-crystal polymer networks, *Materials*, **6**, 116-142.

28. Barberá, J., Jiménez, J., Laguna, A., Oriol, L., Pérez, S., Serrano, J. L. (2006) Cyclotriphos-phazene as a dendritic core for the preparation of columnar supermolecular liquid crystals, *Chem. Mater.*, **18(23)**, 5437–5445.

29. Alam, M. Z., Shibahara, A., Ogata, T., Kurihara, S. (2011) Synthesis of azobenzene-functionalised star polymers via RAFT and their photoresponsive properties, *Polymer*, **52**, 3696–3703.

30. Sarkar, D. D., Deb, R., Chakraborty, M., Nandiraju, V. S. R. (2012) Synthesis of achiral four-ring unsymmetrically substituted toluene

derived liquid crystals with a polar end group, *Liq. Cryst.*, **39(8)**, 1003–1010.

31. Jamain, Z., Khairuddean, M., Zulbaharen, N. N., Chung, T. K. (2019) Synthesis, characterization and determination of mesophase transition of azo-azomethine derivatives with different terminal chain lengths, *Malaysian Journal of Chemistry*, **22**, 73–85.

32. Rong, Y., Wentian, H., Liang, X., Yan, S., Jinchun, L. (2015) Synthesis, mechanical and fire behaviours of rigid polyurethane foam with a reactive flame retardant containing phosphazene and phosphate, *Polym. Degrad. Stab.*, **122**, 102–109.

33. Jamain, Z., Khairuddean, M., Saidin, S. A. (2019) Synthesis and characterization of 1,4-phenylenediamine derivatives containing hydroxyl and cyclotriphosphazene as terminal group, *J. Mol. Struct.*, **1186**, 293–302.

34. Foster, E. J., Jones, R. B., Lavigueur, C., Williams, V. E. (2006) Structural factors controlling the self-assembly of columnar liquid crystals. *J. Am. Chem. Soc*., **128**, 8569–8574.

35. Jeong, M. J., Park, J. H., Lee, C., Chang, J. Y. (2006) Discotic Liquid Hydrazone Compounds: Synthesis and Mesomorphic Properties, *Org. Lett.*, **8**, 2221–2224.

36. Dixit, S., Intwala, K. (2016) Study of novel thermotropic liquid crystals with lateral nitro substituent, *Liq. Cryst.*, **631(1)**, 1–8.

37. Li, Q., Huang, R., Xiong, S., Xie, X. (2012) Synthesis, mesophase behaviour and design principles for discotic liquid crystals of phenyl ethynylene macrocycles with intraannular flexible chains, *Liq. Cryst.*, **39**, 249–258.

38. Nagaveni, N. G., Roy, A., Prasad, V. (2012) Achiral bent-core azo compounds: Effect of different types of linkage groups and their direction of linking on liquid crystalline properties, *J. Mater. Chem.*, **18**, 8948–8959.

39. Selvarasu, C., Kannan, O. (2016) Effect of azo and ester linkages on rod shaped Schiff base liquid crystals and their photophysical investigations, *J. Mol. Struct.*, **1125**, 234–240.

40. Thaker, B. T., Patel, P. H., Vansadiya, A. D., Kanojiya, J. B. (2009) Substitution effects on the liquid crystalline properties of thermotropic liquid crystals containing Schiff base chalcone linkages. *Mol. Cryst. Liq. Cryst.*, **515**, 135–147.

41. Jamain, Z., Khairuddean, M., Guan-Seng, T. (2020) Synthesis of novel liquid crystalline and fire retardant molecules based on six-armed cyclotriphosphazene core containing Schiff base and amide linbking units, *RSC Adv.*, **10(48)**, 28918-28934.

42. Wan, W., Guang, W. J., Zhao, K. Q., Zheng, W. Z., Zhang, L. F. (1998) Calamitic organometallic liquid crystals with a terminal metal. Synthesis and liquid crystal properties of dicarbonylrodhium(I) b-diketonate complexes. *J. Organometallic Chem*., **557**, 157–161.

43. Jamain, Z., Khairuddean, M., Guan-Seng, T. (2020) Synthesis of new star-shaped liquid crystalline cyclotriphosphazene derivatives with fire retardancy bearing amide-azo and azo-azo linking units, *Int. J. Mol. Sci.*, **21**, 4267.

44. Galewski, Z., Coles, H. J. (1999) Liquid crystalline properties and phase situations in 4-chlorobenzylidene-4′-alkylanilines. *J. Mol. Liq*., **79**, 77–87.

45. Lai, C. K., Liu, H. C., Li, F. J., Cheng, K. L., Sheu, H. S. (2005) Heterocyclic Benzoxazole-Based Liquid Crystals, *Liq. Cryst.*, **32**, 85–94.

46. Jamain, Z., Omar, N.F., Khairuddean, M. (2020) Synthesis and determination of thermotropic liquid crystalline behaviour of cinnamaldehyde-based molecules with two Schiff base linking units, *Molecules*, **25**, 3780.